AGU PUBLICATIONS

Geophysical Research Letters

RESEARCH LETTER
10.1002/2018GL077098

Orography and the Boreal Winter Stratosphere: The Importance of the Mongolian Mountains

R. H. White[1,2], D. S. Battisti[2], and A. Sheshadri[3]

[1] JISAO, University of Washington, Seattle, WA, USA, [2] Department of Atmospheric Sciences, University of Washington, Seattle, WA, USA, [3] Department of Applied Physics and Applied Mathematics, Columbia University, New York, NY, USA

Key Points:
- The Rossby refractive index can provide a positive feedback on stratospheric zonal wind changes via altered wave propagation pathways
- The Mongolian mountains have twice the impact on stratospheric flow than the Tibetan plateau and Himalayas
- Sudden stratospheric warmings dramatically reduce in frequency without the Mongolian mountains

Supporting Information:
- Supporting Information S1

Correspondence to:
R. H. White,
rachel.white@cantab.net

Citation:
White, R. H., Battisti, D. S., & Sheshadri, A. (2018). Orography and the boreal winter stratosphere: The importance of the Mongolian mountains. *Geophysical Research Letters*, *45*, 2088–2096. https://doi.org/10.1002/2018GL077098

Received 10 OCT 2017
Accepted 1 FEB 2018
Accepted article online 8 FEB 2018
Published online 26 FEB 2018

Abstract The impact of mountains on stratospheric circulation is explored using the Whole Atmosphere Community Climate Model. The "Mongolian mountains" decrease the boreal winter stratospheric jet strength by ~1/3 and increase the frequency of major sudden stratospheric warmings from 0.08 year^{-1} to the observed 0.60 year^{-1}. These changes are twice the magnitude of the impacts of the Tibetan plateau and Himalayas. Consistent with the decrease in the zonal jet, there is enhanced Eliassen-Palm flux convergence; this is predominantly from changes in wave propagation pathways through changes to the upper troposphere circulation, not from an increased amplitude of planetary waves reaching the stratosphere. The Mongolian mountains have the greater impact on upper tropospheric circulation due to their meridional location. The Rocky Mountains have no significant impact on the stratospheric jet. Changes in wave propagation in response to the Mongolian mountains are similar to those associated with major sudden stratospheric warming events in observations.

Plain Language Summary The stratosphere is a layer of the atmosphere far from the Earth's surface (10–50 km above the surface), but changes in stratospheric circulation, particularly events known as sudden stratospheric warmings, affect the weather and climate at the surface. By flattening individual mountain regions in a climate model that extends from the Earth's surface far past the stratosphere, we study the effects of mountains on stratospheric circulation and the frequency of sudden stratospheric warming events. We find that the presence of the Mongolian mountains weakens the stratospheric jet by a third of its strength and creates 6 times more warming events as there would be without these mountains. The impact of the Mongolian mountains is about twice as large as the impact of the larger and more expansive Tibetan plateau and Himalaya. Mountains are a source of planetary-scale atmospheric waves that propagate upward into the stratosphere; we find that the mountain effect on the stratosphere is largely because the mountains alter the pathway that all waves take as they propagate toward the stratosphere, through the influence the mountains have on circulation lower down in the atmosphere. We find similar anomalous wave propagation during sudden warming events in the model and observations.

1. Introduction

Radiative cooling during the long polar night leads to a strong equator-pole temperature gradient in the winter stratosphere. In thermal wind balance with this temperature gradient exists a strong westerly jet, the stratospheric polar vortex. The structure and dynamics of the polar vortex are vital in setting the distributions of trace gases such as ozone. Observational (e.g., Baldwin & Dunkerton, 1999, 2001) and modeling studies (Gerber et al., 2009; Kushner & Polvani, 2004; Polvani & Kushner, 2002; Sheshadri et al., 2015) have established that variability in the polar vortex can influence the troposphere, all the way to the Earth's surface, on time scales relevant to both weather and climate.

Major sudden stratospheric warming events (SSWs), in which the westerlies in the vortex reverse and the stratospheric polar temperature warms rapidly, occur about every other winter in the Northern Hemisphere (e.g., Charlton & Polvani, 2007; Matsuno, 1971). Only one such event has occurred in the observational record in the Southern Hemisphere (e.g., Newman & Nash, 2005), where the vortex is colder and stronger than its Arctic counterpart (e.g., Waugh & Polvani, 2010). These hemispheric differences are thought to be due to interhemispheric differences in the amplitude of planetary waves generated in the troposphere. Sources of such planetary-scale waves include topography (Charney & Eliassen, 1949), land-sea heating contrasts

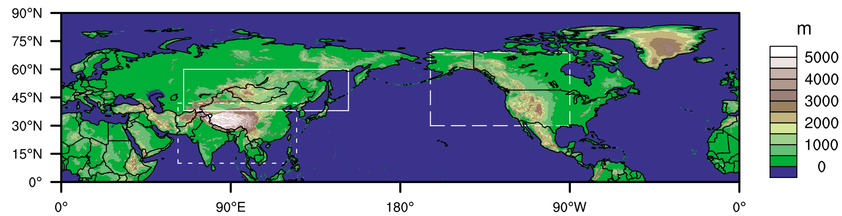

Figure 1. Map of Northern Hemisphere orography, with flattened regions outlined with white boxes. "Tibet" in short dashed line; "Mongolia" in solid line, and "Rockies" in long dashed line.

(Smagorinsky, 1953), and the nonlinear interactions of synoptic-scale eddies (Scinocca & Haynes, 1998). Only the longest (planetary-scale) waves can propagate into the winter stratosphere (Charney & Drazin, 1961), where they break, perturbing the flow away from radiative equilibrium.

Previous studies have explored the impact of the location, wave number, and amplitude of idealized orography on the variability of stratospheric circulation (Gerber & Polvani, 2009; Sheshadri et al., 2015). We use an alternative approach in the present study: starting with a full general circulation model, we examine for the first time the impact of specific orographic features (e.g., the Tibetan Plateau) on the stratosphere, by flattening orography in localized regions within the model. These experiments suggest that the influence of orography is primarily via its influence on wave pathways rather than wave amplitudes. In this paper we first describe the model, the three experiments, and our analysis methods. We evaluate our control simulation, before showing the effects of individual orographic regions on zonal mean stratospheric flow, including Eliassen-Palm (EP) fluxes and their divergence. Orography-induced anomalies in EP flux divergence are diagnosed by studying wave amplitudes and pathways, before the impact of orography on SSWs is presented. We highlight similarities in EP flux pathways between orography-induced anomalies and those associated with SSWs in the model and observations.

2. Model, Experiments, and Analysis Methods

2.1. WACCM Model

To investigate the effects of orography on stratospheric circulation, we use the Whole Atmosphere Community Climate Model (WACCM) within the CESM1.0.6 framework (Marsh et al., 2013). The WACCM has 66 vertical levels extending from the surface to 5.1×10^{-6} hPa and reproduces the observed climatology and variability of stratospheric circulation reasonably well (de la Torre et al., 2012; Marsh et al., 2013). We use a horizontal resolution of 2.5° longitude by 1.9° latitude and include interactive chemistry with emissions from the year 2000. Sea surface temperatures are fixed to a monthly mean climatology from the merged Hadley NOAA Optimum Interpolation (NOAA/OI) data set (Hurrell et al., 2008). See Marsh et al. (2013), and references therein, for more details on the WACCM.

2.2. Experiments

We perform a control simulation (CTL) with all present-day orography, and three experiments with localized regions of Earth's orography flattened. Each simulation runs for 40 years after a 1 year spin-up. Figure 1 shows the regions of orography we focus on: the simulation with orography flattened within the solid white box we denote "No Mongolia," the short-dashed box "No Tibet," and the long-dashed box "No Rockies." The orography flattening is Gaussian weighted at the edges to avoid creating sharp horizontal gradients in orography. In addition to diverting the large-scale flow, orography impacts circulation through subgrid scale processes, including gravity wave drag and an increase in surface roughness. In WACCM, these subgrid scale processes are parameterized through two variables, SGH and SGH30; we set these to 30 and 10 m, respectively, in the flattened regions (approximate values for regions of low orography in Asia; the original values reached up to 1,000 and 500 m, respectively). See White et al. (2017) for further details of the orography flattening. The impact of each mountain region is found as the difference from the CTL experiment, for example, "Impact of Mongolia" = CTL minus No Mongolia. We focus on December–February (DJF), when the coupling between the troposphere and stratosphere is strongest (Kidston et al., 2015) and the majority of SSWs occur (Butler et al., 2017; Charlton & Polvani, 2007).

2.3. Analysis Methods

We analyze our experiments through study of the zonal mean variables: zonal wind ($\overline{u}$; overbar denotes zonal mean), EP fluxes (Eliassen & Palm, 1961), and Rossby wave refractive index (e.g., Hoskins & Karoly, 1981).

We compare results from the CTL simulation to those from daily averages of 6-hourly ERA-Interim reanalysis data at 0.75° resolution (Dee et al., 2011).

EP flux vectors show the propagation of zonal mean wave activity (Andrews & McIntyre, 1976; Edmon et al., 1980; Eliassen & Palm, 1961), while the EP flux divergence gives a measure of the acceleration of zonal mean flow by the waves. We calculate EP fluxes and their divergence on 60 pressure levels from 1,000 to 0.001 hPa using daily data and then take the climatological DJF mean. For display of the EP flux vectors we follow the scaling of Edmon et al. (1980) for log-pressure coordinates, omitting the factor of $2\pi a^2/g$ (where a is the Earth's radius), and then divide by the square root of 1,000/pressure (Taguchi & Hartmann, 2006).

To study the propagation pathways of wave activity, we use a qualitative interpretation of the quasi-geostrophic Rossby refractive index for stationary waves, calculated as an equivalent stationary wave number: $K_S^2 = \overline{q}_y/\overline{u} - f_0^2/4\overline{N}^2 H^2$, where q_y is the meridional gradient of potential vorticity, f_0 the Coriolis parameter, N the stratification and H the scale height (e.g., Andrews et al., 1987; Hoskins & Karoly, 1981; Hu & Tung, 2002; Karoly & Hoskins, 1982). We calculate K_S on daily data, before taking the climatological DJF mean; imaginary values of K_S are treated as missing in the time averaging. Waves are refracted toward regions of greater K_S (Hoskins & Ambrizzi, 1993; Karoly & Hoskins, 1982), and thus changes in K_S gradients alter wave pathways. In regions where the zonal and meridional wave numbers k and l are such that $k^2 + l^2 \geq K_S^2$, the vertical wave number is imaginary, and thus vertical propagation of waves is inhibited (Hoskins & James, 2014; Li et al., 2007). Regions of greater K_S therefore allow waves with larger k and l to propagate vertically.

We use the definition of SSWs of Charlton and Polvani (2007): a major SSW occurs when $\overline{u}$ at 60°N and 10 hPa becomes easterly during November–March, after an interval of 20 or more consecutive days with westerly winds. We consider only major SSWs in this paper. Final warmings, identified as when $\overline{u}$ does not return to westerly for at least 10 consecutive days before 30 April, are excluded. SSWs can be categorized as splits, during which the polar vortex splits into two distinct pieces, and displacements, in which the vortex is displaced away from the pole (Charlton & Polvani, 2007). We categorize each SSW using a subjective analysis of daily geopotential height fields at 10 hPa from 5 days before to 10 days after the date when $\overline{u}$ at 60°N and 10 hPa first becomes easterly: if on any day the geopotential height shows two distinct vortices of similar magnitude then the event is considered a split, otherwise it is classified as a displacement (Charlton & Polvani, 2007; de la Torre et al., 2012).

3. Results

3.1. Control Experiment (CTL)

Values of $\overline{u}$ and EP flux divergence from the CTL simulation are shown in Figure 2a, with the corresponding K_S and EP flux vectors in Figure 2e. The mean circulation is almost identical to that described by Richter et al. (2010) and Marsh et al. (2013) - zonal mean winds and temperatures in boreal winter agree relatively well with observations. There is a cold pole bias, leading to a winter vortex that initiates too early and persists for too long (see Figure S1 in the supporting information) which may affect the stratospheric response to orography toward the beginning and end of winter. EP flux divergence (Figure 2a) and vectors (Figure 2e) agree well with those from the NCEP/NCAR reanalysis (Li et al., 2011), as does the distribution of K_S in Figure 2e (Li et al., 2007). For a detailed discussion of model biases, see Richter et al. (2010) and Marsh et al. (2013).

We evaluate stratospheric variability in the CTL simulation through SSW frequency and histograms of DJF daily $\overline{u}$ at 60°N, 10 hPa. Our CTL simulation has 0.60 ($\pm$0.09) SSWs per year, consistent with previous results (de la Torre et al., 2012), and values from reanalysis data (Charlton & Polvani, 2007); however, the ratio of splits to displacements is 1:4, in contrast to the observed ratio of approximately 1:1.2 (Charlton & Polvani, 2007). This bias is consistent with an overestimation of wave number 1 and underestimation of wave number 2, as found by de la Torre et al. (2012), and shown in Figure S2. We also calculate the frequency distribution of daily $\overline{u}$ values at 60°N, 10 hPa to further evaluate variability: the CTL simulation reproduces the ERA-Interim distribution relatively well (see Figure S3 in the supporting information).

3.2. Flattened Orography Experiments

Flattening orography results in substantial differences in stratospheric flow from October to May, with the greatest differences in November–December (see Figure S1). The impact of orography on DJF zonal mean circulation is shown in Figures 2b–2d and 2f–2h. Contrary to expectations based on mountain heights, but consistent with tropospheric responses (White et al., 2017), the Mongolian mountains have the largest impact on stratospheric flow. The effect of the Mongolian (Tibetan) mountains is to decrease $\overline{u}$ by up to 21 (11) m s^{-1},

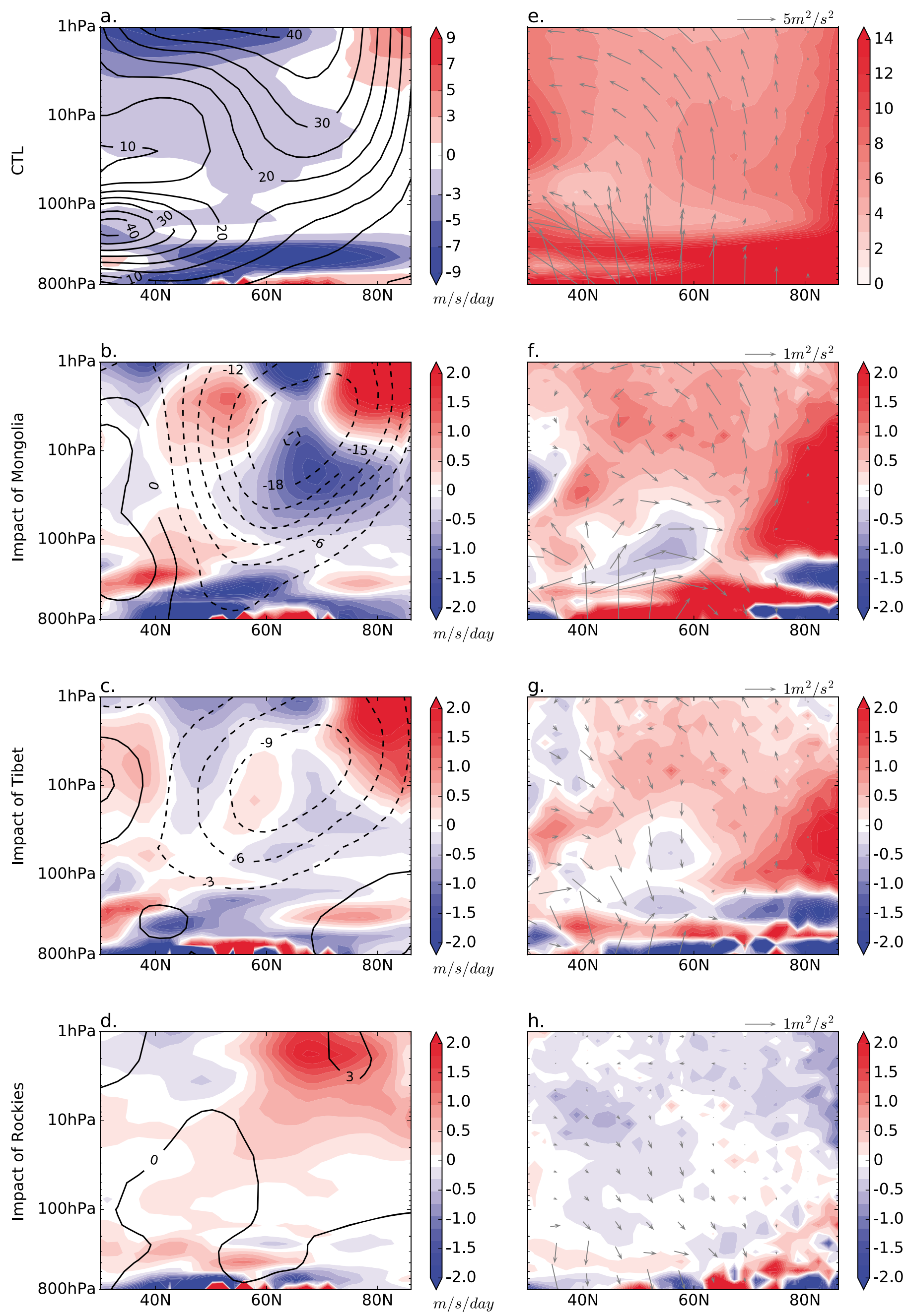

Figure 2. (a) DJF zonal mean zonal wind (black contours; dashed indicating negative) and Eliassen-Palm (EP) flux divergence (colored shading) for the CTL simulation; (e) EP flux vectors (arrows, $m^2\ s^{-2}$) and K_S for the CTL simulation. Subsequent rows are as in the top row but for changes due to the Mongolian mountains (b, f), Tibetan mountains (c, g), and the Rocky Mountains (d, h). The EP flux is divided by the square root of 1,000/pressure to aid visualization; the scale arrow is for pressure = 1,000 hPa. Due to scaling of arrows, EP flux vectors should not be used to estimate divergence.

while the Rockies produce no significant zonal wind changes (Figures 2b–2d). The stratospheric jet zonal wind changes are in thermal wind balance to within 15% (not shown).

The mountain-induced changes in EP flux divergence (Figures 2b–2d) are generally consistent with the changes in $\overline{u}$: the Mongolian and Tibetan mountains both produce anomalous convergence (i.e., negative divergence) near the region of largest zonal wind decrease. Analysis of the individual terms in the EP divergence equation shows that changes in horizontal divergence dominate the response to Mongolia, while both vertical and horizontal divergence changes are important for the Tibetan response (not shown). In contrast to the Asian orography, the Rocky Mountains slightly increase EP flux divergence in the stratospheric jet region.

Orography is a significant source of gravity waves, which can transport momentum into the stratosphere; however, such waves are not resolved in this climate model. Orography-induced changes in the parameterized impact of gravity waves on zonal winds in the stratosphere (obtained as a direct output of the WACCM model) are generally in the opposite direction to the zonal wind forcing from the resolved EP fluxes, consistent with the "compensation mechanism" discussed by Cohen et al. (2013). Orography-induced changes in gravity wave forcing are centered above 10 hPa poleward of 50°N (see Figure S4), and thus, unresolved waves are not a dominant forcing of the changes in the stratospheric jet we study here, although they have a strong influence higher up in the atmosphere.

3.3. Impacts on Wave Activity

Orography-induced anomalies in EP flux divergence can be caused either by a change in wave activity amplitude, or by changes in wave propagation pathways. If changes in wave amplitude were the dominant cause of the orography-induced anomalies in EP flux divergence, then the pattern of anomalous EP fluxes would be nearly identical to that in the control just with reduced amplitude. Figures 2f and 2g show that near the band of latitudes spanned by the mountains (∼30–55°N), the presence of the Mongolian or Tibetan mountains produces a strong increase in wave activity propagating upward from the surface into the upper troposphere; however, the orography-induced EP flux anomalies have generally different propagation pathways from the troposphere to the upper stratosphere than the climatology (cf. Figures 2f and 2g with Figure 2d). Mountains thus also induce changes in wave propagation paths. Additionally, we find that orography-induced anomalies in wave amplitudes for Z at 10 hPa (for wave numbers $k = 1, 2$) are inconsistent with the changes in EP flux divergence across the three experiments (see Figure S2), further suggesting that the orography-induced changes in EP flux divergence cannot be attributed solely to the orography acting as an additional source of Rossby waves.

Since changes in wave amplitude alone cannot explain the changes in EP flux divergence, we examine orography-induced anomalies in K_S (Figures 2f–2h), which can alter wave propagation pathways and thus EP flux divergence. Between ∼55–80°N and ∼200–10 hPa the Mongolian mountains induce a change in K_S with a positive poleward gradient. This would act to deflect wave activity poleward relative to the control case and thus cause an increase in EP flux convergence poleward of ∼50°N, consistent with the orography-induced anomalies in EP flux vectors and convergence in this region (Figure 2b). The mountains also generally increase K_S in the stratosphere, which will allow more wave activity to propagate vertically into the stratosphere, where it can converge. Orography-induced changes in K_S are primarily due to changes in the meridional gradient of potential vorticity ($\overline{q_y}$) and the zonal wind ($\overline{u}$), and not changes in buoyancy ($f_0^2/4N^2H^2$) (not shown).

The change in K_S due to the Tibetan mountains has a similar spatial structure to the changes due to the Mongolian mountains, but are of smaller magnitude (Figure 2g), consistent with the smaller changes in EP flux divergence and $\overline{u}$. Compared to Mongolia or Tibet, the Rockies have a much smaller impact on K_S (Figure 2h), consistent with the small impact of the Rockies on the stratospheric zonal wind.

These results indicate that changes in refractive index are of central importance for the impact of orography on the wintertime stratospheric circulation. The changes in K_S stem from changes in the circulation of the upper troposphere associated with the various orographic features. As shown by White et al. (2017), the Mongolian mountains have a greater impact on the upper tropospheric wintertime circulation than the Tibetan plateau.

3.4. Impacts on Major Sudden Stratospheric Warmings and Stratospheric Variability

By changing the climatological mean flow and propagation of wave activity, the presence of mountains affects the frequency of major SSWs. The first column of Table 1 shows the SSW frequency in the different experiments, using a standard definition of SSWs (see section 2.3). Without the Mongolian mountains, the frequency of SSWs drops from 0.6 SSWs per year to 0.08. Removing the Tibetan mountains also reduces the frequency of SSWs, albeit weakly compared to the Mongolian mountains, while removing the Rockies has no statistically significant impact. The presence of mountains causes no significant change in the date of the seasonal vortex breakdown at the end of polar winter, as defined by Black and McDaniel (2007) (at 10 mb); the delay in the switch from westerlies to easterlies when the orography is not present, as seen in Figure S3 in the supporting information, is not statistically significant with 40 years of data. Reductions in both displacement and split SSWs occur when the Mongolian or Tibetan mountains are removed; however, given the strong

10.1002/2018GL077098

Table 1
Summary of SSW Frequency in the CTL Simulation and the Three "No Mountain" Experiments

Experiment	SSW frequency	$SSW_{\Delta\overline{u}}$ frequency
CTL	0.60 (0.09)	0.60 (0.09)
No Mongolia	0.08 (0.04)	0.30 (0.08)
No Tibet	0.28 (0.07)	0.40 (0.09)
No Rockies	0.70 (0.10)	0.63 (0.09)

Note. The second column is the frequency of SSWs based on the standard definition. The third column is the $SSW_{\Delta\overline{u}}$ frequency: SSWs defined as a decrease of $\Delta\overline{u} = 28.1$ m s^{-1} from the DJF climatological mean flow for each simulation; see text for further details. Values in parentheses give 1 standard error based on Charlton and Polvani (2007).

bias toward displacement events in this version of the model (and subsequently the small number of split events), the effect of mountains on the ratio of splits to displacements cannot be robustly determined.

This decrease in SSW frequency could be caused by a decrease in the variability of $\overline{u}$ when mountains are removed, or simply to the increased climatological mean flow (with no change in variability) as $\overline{u}$ must decrease by a larger value to reach the 0 m s^{-1} threshold. To study the relative importance of these two aspects, we create a new SSW definition to remove the influence of the change in climatological flow: instead of a fixed $\overline{u}$ threshold of 0 m s^{-1}, we define an SSW as a specified deviation in $\overline{u}$ ($\Delta\overline{u}$) from the DJF climatological value for each simulation. We take $\Delta\overline{u}$ to be the difference between the DJF climatological mean value in the CTL simulation (28.1m s^{-1}) and 0 m s^{-1}. By this new definition, the frequency of SSWs only drops from 0.6 per year in the CTL simulation to 0.30 per year when the Mongolia mountains are removed, while the standard definition renders 0.08 per year without the Mongolian mountains (compare columns in Table 1). Thus, approximately half of the decrease in SSW frequency when the mountains are removed is due to a simple increase in the mean $\overline{u}$, with the other half from a decrease in the variability of $\overline{u}$.

Lastly, we examine how the anomalies associated with the presence of the Mongolian mountains compare with anomalies associated with SSWs in the CTL simulation and ERA-Interim reanalysis data. We show the difference in K_S and EP fluxes in winters with at least one SSW relative to winters with no SSWs in WACCM and observations (Figures 3a and 3c). We also calculate a composite of K_S and EP fluxes during all days in SSW maturation phases, defined as the 10 days prior to the minimum in $\overline{u}$ at 60°N, 10 hPa (Figures 3b and 3d); this is the period during which $\overline{u}$ is decreasing most rapidly. Three conclusions are drawn from Figure 3. First, the anomalies in K_S and EP fluxes associated with SSWs in WACCM are relatively similar to those in observations (cf. Figures 3a with 3c and 3b with 3d). Second, as expected, the transient anomalies in K_S and EP fluxes due to SSW events have a very similar spatial structure to the seasonal average values associated with winters in

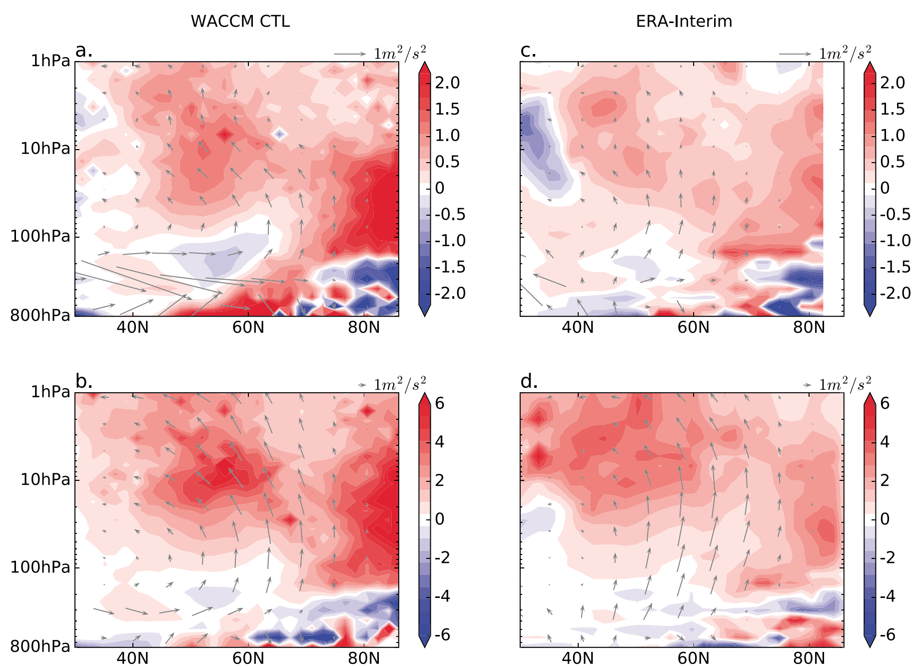

Figure 3. K_S and Eliassen-Palm flux vectors (m^2 s^{-2}) associated with sudden stratospheric warmings (SSWs) in (a, b) CTL and (c, d) ERA-Interim. (a, c) SSW-winter anomalies—composite of all DJF daily values for seasons with at least one SSW minus that for seasons with no SSWs. (b, d) Composite anomalies during the growth phase of SSWs (relative to DJF composite for seasons with no SSWs). All values are calculated on daily data before time averaging. Note changes in scales between top and bottom rows.

which SSW occur relative to winters with no SSWs in both WACCM and observations (cf. Figure 3a with 3b and 3c with 3d; note changes in scales). Finally, there is a high degree of similarity between the response to Mongolia and these SSW-associated anomalies (cf. Figure 3 with Figure 2f), with poleward EP fluxes in the upper troposphere/lower stratosphere, an increase in vertical EP flux centered around 60°N, and general increases in K_S in the stratosphere with a local maximum near the pole between 200 and 10 hPa. Corresponding changes in $\overline{u}$ and EP flux divergence are shown in Figure S5. Our results are consistent with the conclusion that SSWs are associated anomalous poleward propagation of wave activity, and with K_S conditions that are more conducive to this propagation pathway.

4. Discussion and Conclusions

This study uses the WACCM model to examine the relative importance of the three major NH orographic features in shaping Northern Hemisphere (NH) stratospheric circulation. The Mongolian mountains, located north of the higher altitude and more expansive Tibetan plateau and Himalaya, have the greatest impact on NH wintertime stratospheric flow, reducing the strength of the stratospheric jet by a third. The impact of the Tibetan plateau and Himalaya is similar, although with half the magnitude. The Rocky Mountains have no significant impact on stratospheric flow. The frequency of SSWs decreases when the Mongolian or Tibetan mountains are removed, partially because the threshold of 0 m s^{-1} is more difficult to reach from a faster mean flow, and partially because the variability of $\overline{u}$ decreases without the mountains.

The orography-induced changes in zonal mean zonal wind are consistent with anomalous EP flux divergence, indicating that resolved wave-mean-flow interactions are key for the stratospheric response to orography. The presence of mountains has a strong impact on wave propagation paths, which affects the EP flux divergence. Orography-induced changes in K_S, the Rossby refractive index, exhibit meridional gradients that should increase poleward propagation of waves, increasing convergence. We conclude that orographically induced changes in background (upper tropospheric) flow, not changes in the amplitude of stratospheric transient or stationary wave activity (e.g., Plumb, 1981), are the dominant cause of mountain-induced changes in EP flux divergence.

The decrease in $\overline{u}$ from the increased EP flux convergence will generally act to reinforce the local changes in refractive index. This highlights a positive feedback mechanism in troposphere-stratosphere coupling: the K_S anomalies associated with initial decreases in $\overline{u}$ alter wave propagation pathways, leading to greater EP flux convergence in the stratosphere, further slowing winds. Mongolia-induced changes in EP fluxes and refractive index are found to be similar in pattern to anomalies associated with SSWs in the WACCM model and ERA-Interim reanalysis. EP fluxes associated with SSWs also show anomalous poleward propagation in the upper troposphere from 22 days prior to an SSW, with anomalous vertical fluxes centered around 70°N (Limpasuvan et al., 2004), similar to the response we find to the Mongolian mountains. Our results therefore suggest a role for positive K_S feedbacks in SSW events.

Different mountain ranges have substantially different impacts on the stratospheric circulation, with orographic height clearly not the most important factor. White et al. (2017) show that the Mongolian mountains have a stronger impact on the DJF tropospheric jet than the Tibetan plateau, due to the latitudinal distribution of impinging wind, and potential vorticity gradient, both affecting the near-field response strength; and the horizontal distribution of K_S affecting propagation pathways. The peak of the Rocky Mountains lies at a latitude between the Mongolian and Tibetan mountains (Figure 1); however, the Rocky Mountains have no significant impact on stratospheric $\overline{u}$. Whether this is due to the shape of the orography or from zonal variations in flow or wave propagation, is yet to be determined. It is worth noting that Mongolia has a particularly large impact on the upper tropospheric flow in the North Pacific (White et al., 2017), a region thought to be particularly important for SSWs (e.g., Garfinkel et al., 2012). The region over Eastern Asia and the North Pacific has been previously highlighted regarding longitudinal asymmetries in the stratosphere (Kozubek et al., 2015; Šácha et al., 2015).

There is a large hemispheric asymmetry in stratospheric flow, with a slower and more variable jet in the Northern Hemisphere, and SSWs an extremely rare occurrence in the Southern Hemisphere (SH) (Thompson et al., 2005). These differences are typically attributed to differences in orography and/or zonal gradients in diabatic heating (i.e., land-sea distribution). Our results give further insight into the relative importance of these asymmetries: comparison of the mean speed and variability of the SH stratosphere wintertime (JJA) jet with those of the NH wintertime jet in a simulation without any orography worldwide suggests that the mean speed of the jet is impacted predominantly by the orography, while the variability about this mean is affected both by the orography and the zonal gradients in diabatic heating (see Figure S6 in the supporting information).

Along with the changes in stratospheric circulation, these model experiments also show that springtime ozone over the NH pole (70–90°N) increases by up to 80 DU (20%) with the presence of the Mongolian mountains (see Figure S7 in the supporting information). This mountain effect is approximately half the magnitude of the SH ozone reduction since the 1950s (Solomon, 1999). This mountain-induced increase in ozone is likely a combination of chemistry and dynamics: the mountain-induced increase in stratospheric polar temperatures results in reduced ozone loss from ozone-depleting substances such as CFCs (Solomon, 1999), while an increase in the Brewer-Dobson circulation suggests an increase in troposphere-stratosphere transport of ozone (not shown). Further work investigating the role of mountains on stratospheric ozone may be of interest to paleoclimate studies.

Our results show that the boreal winter stratospheric circulation is significantly shaped by the presence of the Mongolian mountains, due to their impact on the upper tropospheric mean flow and subsequent impacts on wave propagation pathways. Thus, the stratospheric circulation, and its variability, may be sensitive to changes in the flow impinging on Mongolia under past climates with differing orography, such as Last Glacial Maximum conditions, or in a future, warmer, climate.

Acknowledgments
The authors thank Mike Wallace, Lorenzo Polvani, Ted Shepherd, Dennis Hartmann, and Petr Šácha for useful discussions on this work, as well as two anonymous reviewers. R. H. W. was supported by the Joint Institute for the Study of the Atmosphere and Ocean (JISAO), and the Atmospheric Sciences department, at the University of Washington. D. S. B. was supported by a grant from the Tamaki Foundation. A. S. was supported by the Simons Foundation through Junior Fellow award 354584. The CESM project is supported by the National Science Foundation and the Office of Science (BER) of the U.S. Department of Energy. ERA-Interim reanalysis data were downloaded from the ECMWF using MARS.

References

Andrews, D. G., & McIntyre, M. E. (1976). Planetary waves in horizontal and vertical shear: The generalized Eliassen-Palm relation and the mean zonal acceleration. *Journal of the Atmospheric Sciences*, *33*(11), 2031–2048. https://doi.org/10.1175/1520-0469(1976)033<2031:PWIHAV>2.0.CO;2

Andrews, D. G., Holton, J. R., & Leovy, C. B. (1987). *Middle atmopshere dynamics* (489 pp.). New York: Academic Press.

Baldwin, M. P., & Dunkerton, T. J. (1999). Propagation of the Arctic Oscillation from the stratosphere to the troposphere. *Journal of Geophysical Research*, *104*(D24), 30,937–30,946. https://doi.org/10.1029/1999JD900445

Baldwin, M. P., & Dunkerton, T. J. (2001). Stratospheric harbingers of anomalous weather regimes. *Science*, *294*(5542), 581–584. https://doi.org/10.1126/science.1063315

Black, R. X., & McDaniel, B. A. (2007). The dynamics of Northern Hemisphere stratospheric final warming events. *Journal of the Atmospheric Sciences*, *64*(8), 2932–2946. https://doi.org/10.1175/JAS3981.1

Butler, A. H., Sjoberg, J. P., Seidel, D. J., & Rosenlof, K. H. (2017). A sudden stratospheric warming compendium. *Earth System Science Data*, *9*(1), 63–76. https://doi.org/10.5194/essd-9-63-2017

Charlton, A. J., & Polvani, L. M. (2007). A new look at stratospheric sudden warmings. Part I: Climatology and modeling benchmarks. *Journal of Climate*, *20*(3), 449–469. https://doi.org/10.1175/JCLI3996.1

Charney, J. G., & Drazin, P. G. (1961). Propagation of planetary-scale disturbances from the lower into the upper atmosphere. *Journal of Geophysical Research*, *66*, 83–109. https://doi.org/10.1029/JZ066i001p00083

Charney, J. G., & Eliassen, A. (1949). A numerical method for predicting the perturbations of the middle latitude westerlies. *Tellus*, *1*(2), 38–54. https://doi.org/10.1111/j.2153-3490.1949.tb01258.x

Cohen, N. Y., Edwin P. G., & Oliver B. (2013). Compensation between resolved and unresolved wave driving in the stratosphere: Implications for downward control. *Journal of the Atmospheric Sciences*, *70*(12), 3780–3798. https://doi.org/10.1175/JAS-D-12-0346.1

de la Torre, L., Garcia, R. R., Barriopedro, D., & Chandran, A. (2012). Climatology and characteristics of stratospheric sudden warmings in the whole atmosphere community climate model. *Journal of Geophysical Research*, *117*, D04110. https://doi.org/10.1029/2011JD016840

Dee, D. P., Uppala, S. M., Simmons, A. J., Berrisford, P., Poli, P., Kobayashi, S., et al. (2011). The ERA-Interim reanalysis: Configuration and performance of the data assimilation system. *Quarterly Journal of the Royal Meteorological Society*, *137*(656), 553–597.

Edmon, H. J., Hoskins, B. J., & McIntyre, M. E. (1980). Eliassen-Palm cross sections for the troposphere. *Journal of the Atmospheric Sciences*, *37*(12), 2600–2616. https://doi.org/10.1175/1520-0469(1980)037<2600:EPCSFT>2.0.CO;2

Eliassen, A., & Palm, E. (1961). On the transfer of energy in stationary mountain waves. *Geofysiske Publikasjoner*, *22*(3), 1–23. https://doi.org/10.1002/qj.49707934103

Garfinkel, C. I., Butler, A. H., Waugh, D. W., Hurwitz, M. M., & Polvani, L. M. (2012). Why might stratospheric sudden warmings occur with similar frequency in El Niño and La Niña winters? *Journal of Geophysical Research*, *117*, D19106. https://doi.org/10.1029/2012JD017777

Gerber, E. P., & Polvani, L. M. (2009). Stratosphere-troposphere coupling in a relatively simple AGCM: The importance of stratospheric variability. *Journal of Climate*, *22*(8), 1920–1933. https://doi.org/10.1175/2008JCLI2548.1

Gerber, E. P., Orbe, C., & Polvani, L. M. (2009). Stratospheric influence on the tropospheric circulation revealed by idealized ensemble forecasts. *Geophysical Research Letters*, *36*, L24801. https://doi.org/10.1029/2009GL040913

Hoskins, B., & Ambrizzi, T. (1993). Rossby-wave propagation on a realistic longitudinally varying flow. *Journal of the Atmospheric Sciences*, *50*(12), 1661–1671. https://doi.org/10.1175/1520-0469(1993)050<1661:RWPOAR>2.0.CO;2

Hoskins, B. J., & James, I. N. (2014). *Fluid dynamics of the mid-latitude atmosphere*. Hoboken, NJ: John Wiley.

Hoskins, B. J., & Karoly, D. J. (1981). The steady linear response of a spherical atmosphere to thermal and orographic forcing. *Journal of the Atmospheric Sciences*, *38*(6), 1179–1196. https://doi.org/10.1175/1520-0469(1981) 038<1179:tslroa>2.0.co;2

Hu, Y. Y., & Tung, K. K. (2002). Interannual and decadal variations of planetary wave activity, stratospheric cooling, and Northern Hemisphere annular mode. *Journal of Climate*, *15*(13), 1659–1673. https://doi.org/10.1175/1520-0442(2002)015<1659:iadvop>2.0.co;2

Hurrell, J. W., Hack, J. J., Shea, D., Caron, J. M., & Rosinski, J. (2008). A new sea surface temperature and sea ice boundary dataset for the community atmosphere model. *Journal of Climate*, *21*(19), 5145–5153. https://doi.org/10.1175/2008jcli2292.1

Karoly, D. J., & Hoskins, B. J. (1982). Three dimensional propagation of planetary waves. *Journal of the Meteorological Society of Japan. Ser. II*, *60*(1), 109–123. https://doi.org/10.2151/jmsj1965.60.1_109

Kidston, J., Scaife, A. A., Hardiman, S. C., Mitchell, D. M., Butchart, N., Baldwin, M. P., & Gray, L. J. (2015). Stratospheric influence on tropospheric jet streams, storm tracks and surface weather. *Nature Geoscience*, *8*(6), 433–440. https://doi.org/10.1038/ngeo2424

Kozubek, M., Krizan, P., & Lastovicka, J. (2015). Northern Hemisphere stratospheric winds in higher midlatitudes: Longitudinal distribution and long-term trends. *Atmospheric Chemistry and Physics*, *15*(4), 2203–2213. https://doi.org/10.5194/acp-15-2203-2015

Kushner, P. J., & Polvani, L. M. (2004). Stratosphere-troposphere coupling in a relatively simple AGCM: The role of eddies. *Journal of Climate*, *17*(3), 629–639. https://doi.org/10.1175/1520-0442(2004)017<0629:SCIARS>2.0.CO;2

Li, Q., Graf, H.-F., & Giorgetta, M. A. (2007). Stationary planetary wave propagation in Northern Hemisphere winter—Climatological analysis of the refractive index. *Atmospheric Chemistry and Physics*, *7*(1), 183–200. https://doi.org/10.5194/acp-7-183-2007

Li, Q., Graf, H.-F., & Cui, X. (2011). The role of stationary and transient planetary waves in the maintenance of stratospheric polar vortex regimes in Northern Hemisphere winter. *Advances in Atmospheric Sciences*, *28*(1), 187–194. https://doi.org/10.1007/s00376-010-9163-7

Limpasuvan, V., Thompson, D. W. J., & Hartmann, D. L. (2004). The life cycle of the Northern Hemisphere sudden stratospheric warmings. *Journal of Climate*, *17*(13), 2584–2596. https://doi.org/10.1175/1520-0442(2004)017<2584:TLCOTN>2.0.CO;2

Marsh, D. R., Mills, M. J., Kinnison, D. E., Lamarque, J.-F., Calvo, N., & Polvani, L. M. (2013). Climate change from 1850 to 2005 simulated in CESM1(WACCM). *Journal of Climate*, *26*(19), 7372–7391. https://doi.org/10.1175/JCLI-D-12-00558.1

Matsuno, T. (1971). A dynamical model of the stratospheric sudden warming. *Journal of the Atmospheric Sciences*, *28*(8), 1479–1494. https://doi.org/10.1175/1520-0469(1971)028<1479:ADMOTS>2.0.CO; 2

Newman, P. A., & Nash, E. R. (2005). The unusual Southern Hemisphere stratosphere winter of 2002. *Journal of the Atmospheric Sciences*, *62*(3), 614–628. https://doi.org/10.1175/JAS-3323.1

Plumb, R. A. (1981). Instability of the distorted polar night vortex: A theory of stratospheric warmings. *Journal of the Atmospheric Sciences*, *38*(11), 2514–2531. https://doi.org/10.1175/1520-0469(1981)038<2514:IOTDPN>2.0.CO;2

Polvani, L. M., & Kushner, P. J. (2002). Tropospheric response to stratospheric perturbations in a relatively simple general circulation model. *Geophysical Research Letters*, *29*(7), 1114. https://doi.org/10.1029/2001GL014284

Richter, J. H., Sassi, F., & Garcia, R. R. (2010). Toward a physically based gravity wave source parameterization in a general circulation model. *Journal of the Atmospheric Sciences*, *67*(1), 136–156. https://doi.org/10.1175/2009JAS3112.1

Šácha, P., Kuchař, A., Jacobi, C., & Pišoft, P. (2015). Enhanced internal gravity wave activity and breaking over the northeastern Pacific-eastern Asian region. *Atmospheric Chemistry and Physics*, *15*(22), 13,097–13,112. https://doi.org/10.5194/acp-15-13097-2015

Scinocca, J. F., & Haynes, P. H. (1998). Dynamical forcing of stratospheric planetary waves by tropospheric baroclinic eddies. *Journal of the Atmospheric Sciences*, *55*(14), 2361–2392. https://doi.org/10.1175/1520-0469(1998) 055<2361:DFOSPW>2.0.CO;2

Sheshadri, A., Plumb, R. A., & Gerber, E. P. (2015). Seasonal variability of the polar stratospheric vortex in an idealized AGCM with varying tropospheric wave forcing. *Journal of the Atmospheric Sciences*, *72*(6), 2248–2266. https://doi.org/10.1175/JAS-D-14-0191.1

Smagorinsky, J. (1953). The dynamical influence of large-scale heat sources and sinks on the quasi-stationary mean motions of the atmosphere. *Quarterly Journal of the Royal Meteorological Society*, *79*(341), 342–366. https://doi.org/10.1002/qj.49707934103

Solomon, S. (1999). Stratospheric ozone depletion: A review of concepts and history. *Reviews of Geophysics*, *37*(3), 275–316. https://doi.org/10.1029/1999RG900008

Taguchi, M., & Hartmann, D. L. (2006). Increased occurrence of stratospheric sudden warmings during El Niño as simulated by WACCM. *Journal of Climate*, *19*(3), 324–332. https://doi.org/10.1175/JCLI3655.1

Thompson, D. W. J., Baldwin, M. P., & Solomon, S. (2005). Stratosphere–troposphere coupling in the Southern Hemisphere. *Journal of the Atmospheric Sciences*, *62*(3), 708–715. https://doi.org/10.1175/JAS-3321.1

Waugh, D. W., & Polvani, L. M. (2010). Stratospheric polar vortices. In L. M. Polvani, A. H. Sobel, & D. W. Waugh (Eds.), *The stratosphere: Dynamics, transport, and chemistry* (pp. 43–57). Washington, DC: American Geophysical Union. https://doi.org/10.1002/9781118666630.ch3

White, R. H., Battisti, D. S., & Roe, G. H. (2017). Mongolian Mountains matter most: Impacts of the latitude and height of Asian orography on Pacific wintertime atmospheric circulation. *Journal of Climate*, *39*, 4065–4082. https://doi.org/10.1175/JCLI-D-16-0401.1